

Climate of the Past Discussions

Reply to Interactive comment of Anonymous Referee #2 on “Orbitally tuned time scale and astronomical forcing in the middle Eocene to early Oligocene” by T. Westerhold, U. Röhl, H. Pälike, R. Wilkens, P. A. Wilson, and G. Acton.

We thank Anonymous Referee #2 for the critical comments regarding the paleomagnetic interpretation and correlation between ODP Site 1218 and IODP Sites U1333/U1334 as well as the concern about the quality and documentation of paleomagnetic data from ODP Sites 1052, 1172 and 1260.

Please find below our reply to issues Anonymous Referee #2 raised and the corrections we suggest for the manuscript. The original comments are italicized and our responses are in normal font red colored.

Apart from a sentence in the caption of Fig. 2, it is not stated that the magnetic stratigraphies for Sites 1218 and U1334 are “mapped in” from Site U1333. Table S16 in the Pangaea database has a heading that also states that the magnetic stratigraphies for Sites U1334 and 1218 are “mapped in” from Site U1333. This obviously means that the magnetic stratigraphies for Sites U1333, U1334 and 1218 are not independent. The Site U1333 polarity zone boundaries are “mapped into” Sites U1334 and 1218 using the same XRF and other core-scanning data that is used to derive the astrochronologies. The filtered output from the XRF data, that are used to derive the astrochronologies, are certain to correlate from site to site if the site-to-site correlations are based on the magnetostratigraphies (and XRF data), and the XRF data are used to “map in” the magnetostratigraphies from Site U1333 to Sites 1218 and U1334.

The reviewers comment is that the transfer of data from one site to the others is not well enough stated. In the figures 3,4,5 & 7 of the manuscript the U1333 paleomagnetic interpretation is in black and the mapped-in reversal patterns in 1218 and U1334 are in gray. The information in figures 3,4,5 & 7, the heading of table S16 and the cross-reference to the correlation between 1218, U1333 and U1334 of Westerhold et al. 2012 should be sufficient for the reader to understand that the paleomagnetic interpretation of U1333 is mapped onto 1218 and U1334. But, to make this more visible for the reader we added the following to Chapter 4 *Cyclostratigraphic framework*: “Because the correlation between sites can be done with high accuracy and precision (Westerhold et al., 2012), magnetostratigraphy from U1333 is transferred or mapped to 1218 and U1334. This enables to identify the period of prominent cyclicity at all three PEAT records and evaluate the error in astronomically tuned ages for magnetostratigraphic boundaries.”

To show to the reviewer that it is possible to transfer the magnetostratigraphy from U1333 to 1218 and U1334 we plotted three figures (Fig. 1, 2 and 3 of this reply) with the correlation of XRF core scanner derived Fe_2O_3 and CaCO_3 concentrations of the three sites and declination data from U1333 (that subsequently was transferred to the other sites). Uncertainty in the correlation of the high-quality XRF core scanning data and physical property data for the three sites (also see Westerhold et al., 2012 Figure F22) is in the order of centimeters. Uncertainty in the magnetostratigraphic data of U1333 is between ± 0.01 and 0.06 m (given in Table S16). The error increase due to correlation from one site to another is very low. Additionally, in Table S16 the error of the applied

tuned age model is given for each site based on the depth error. The table shows that higher sedimentation rates (U1334) results in a bigger error bar on the absolute age estimates of chron boundaries. This is not surprising because the magnetostratigraphy was established at lower sedimentation rate Site U1333 compared to U1334 (see manuscript Fig. 8). We combined all three age estimates for each chron boundary to calculate a maximum and minimum age to get an impression of the error introduced by tuning of the different sites (actually it is the position of the tie points that determine the error). Please note that the error does not include uncertainties of the orbital solution itself. We think that this gives a more realistic impression than the very tight ages of U1333 alone (Tab. S16).

The reviewer here criticizes as well, if we understand correctly, that due to the mapping of the U1333 magnetostratigraphy to the other sites the filter outputs of sites 1218 and U1334 will give the same result as U1333. This is correct if the filters are applied in the age domain only. To avoid circular reasoning the primary filtering target is the depth domain in the manuscript, as can be seen in almost all figures of the manuscript. Subsequently the mapped in magnetostratigraphies help to identify the dominant cycles present at the different sites. Doing so we use the Cande & Kent 1995 age model that has no astronomical tuned calibration points in the interval of interest.

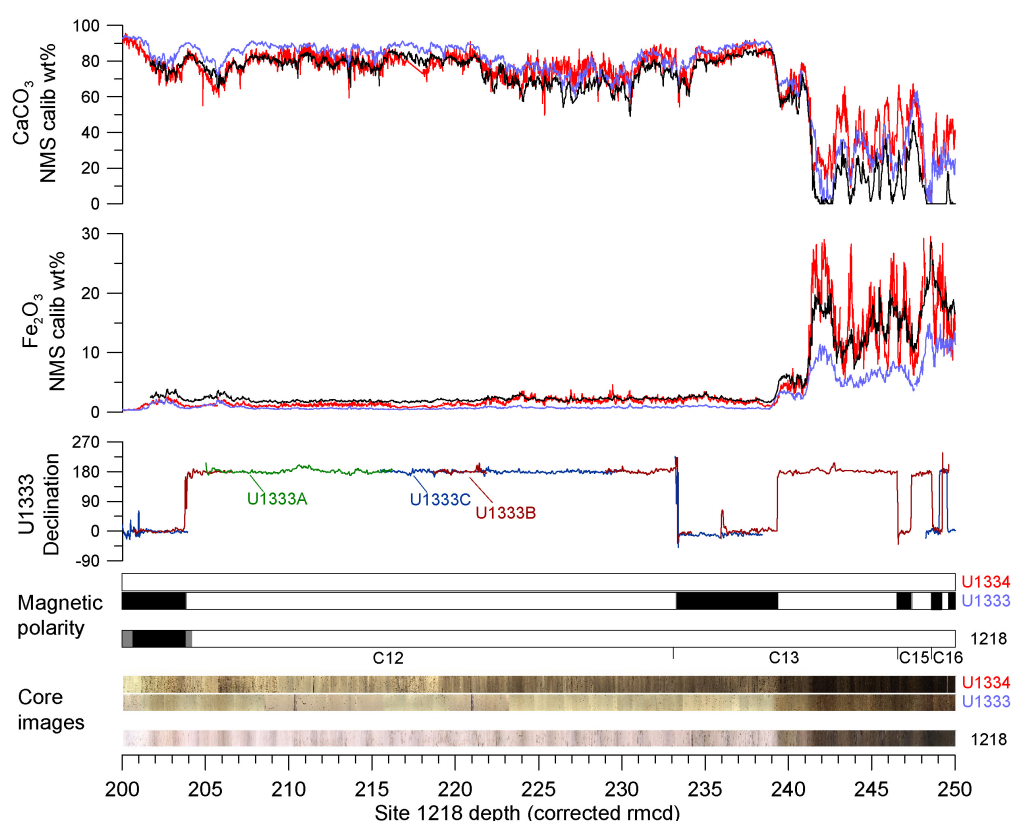


Figure 1. Site-to-site correlation covering magnetostratigraphy C12 to C16 of calibrated Fe and Ca XRF core scanning data from Sites 1218 (black line), U1333 (bright blue line), and U1334 (red) as well as declination data from U1333 (Hole A – green, Hole B – dark red, Hole C – dark blue) on corrected rmcd scale of Site 1218 (Westerhold et al., 2012). Core images for reference.

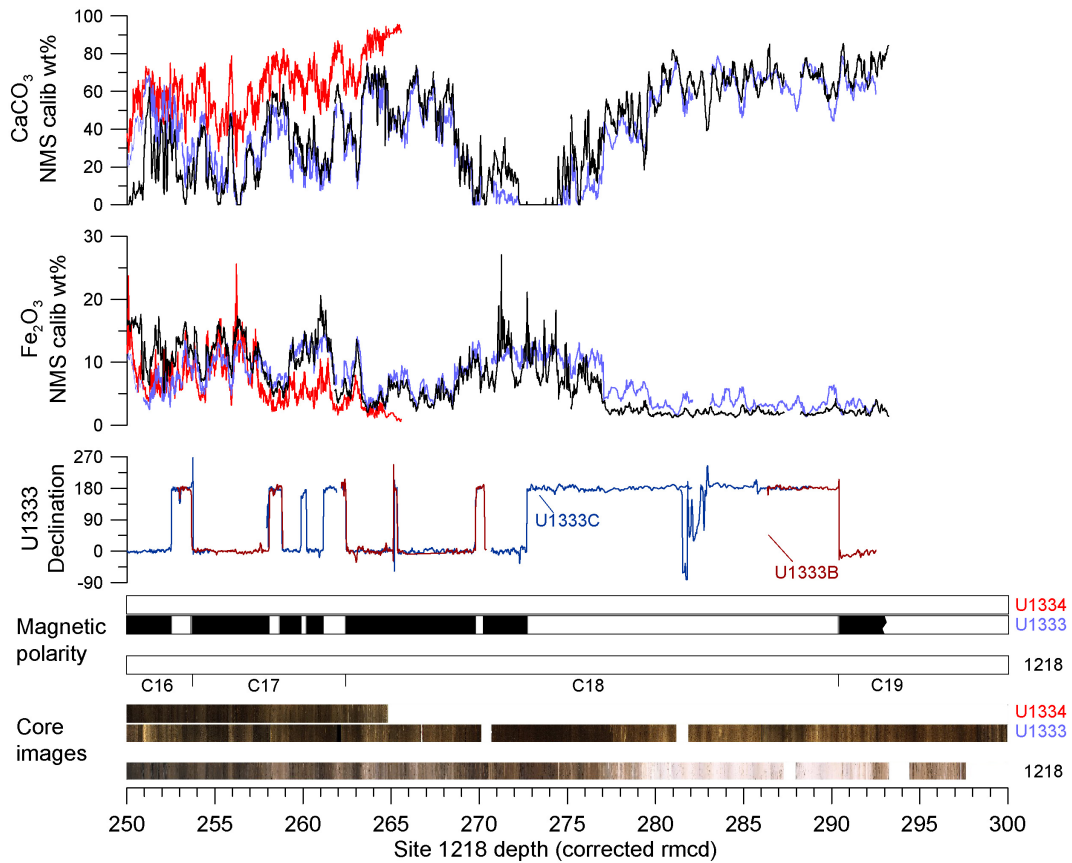


Figure 2. Site-to-site correlation covering magnetochron C16 to C19 of calibrated Fe and Ca XRF core scanning data from Sites 1218 (black line), U1333 (bright blue line), and U1334 (red) as well as declination data from U1333 (Hole B – dark red, Hole C – dark blue) on corrected rmcd scale of Site 1218 (Westerhold et al., 2012). Core images for reference.

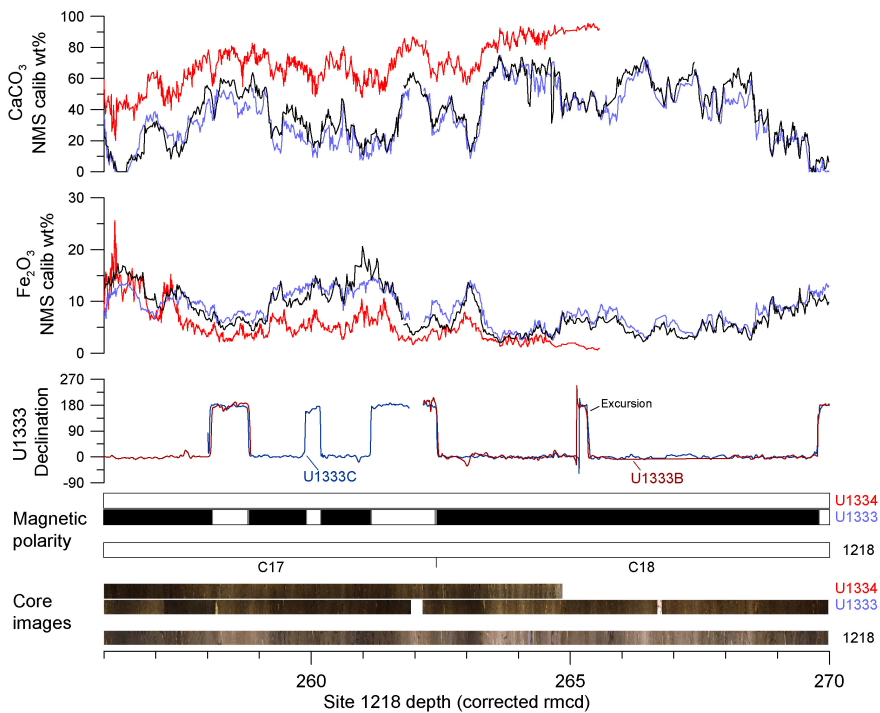


Figure 3. Close-up of Figure 2 from 256 to 270 rmcd.

Turning to Site U1333: The magnetic stratigraphy at Site U1333 for C12n to C20n is presented in the Supplemental Information and in the Pangaea database. Two figures: a demagnetization diagram (Fig. S12) and a plot of VGP latitudes and declinations versus age (Fig. S13) represent the documentation of what appears to be a high-quality and useful magnetic stratigraphy. In the future, particularly if these astrochronologic ages for the GPTS are adopted, those interested in timescales will want to see more details on the Site U1333 magnetic stratigraphies. Although the data are archived in Pangaea, more complete documentation should be included in this paper, or published elsewhere, before publication of the astrochronologies considered here. Statements in the Supplemental Information of this paper such as: "As shown by Pälike et al. (2010) [Shipboard Data], Site U1333 sediments are accurate recorders of the paleomagnetic field..." are misleading because it is not possible to determine this from shipboard data.

The shipboard paleomagnetists provided fairly clear evidence of the stability of the magnetization and clarity of the magnetostratigraphy in the shipboard data but that is non-peer reviewed and perhaps not readily acceptable to all. Most of that is pure data without excessive interpretation and the shipboard data were not controversial or open to vastly different interpretation. The shipboard data are all relatively straightforward. Our intention in the manuscript was to be concise and give sufficient data to see that the magnetostratigraphy is very well resolved. Zijdeveld plots for every sample (thousands of plots), rock magnetic data, and plenty of other information are available upon request from Gary Acton. Providing all that would be too much and probably an extra manuscript. But to better document the quality of the magnetic stratigraphy at U1333 we provide access to the Tables (referee #2 can contact the editor (Andrea Dutton) and request the tables). The data file is also much more than typically provided by paleomagnetists and hopefully enough to prove the good quality of the data to referee #2. (see table at the end of the reply)

An extra Figure S15 (Figure 4a & 4b of this reply) is introduced to the supplement plotting vector demagnetization diagrams and intensity decay plots for a sequence of samples across the Chron C13n/C13r boundary. This sequence shows that the paleomagnetic direction can be very well resolved even for samples only a few centimeters on either side of the reversal boundary (e.g., the reversed polarity sample in Supplementary Figure S15E is only 3 cm below the Chron C13n/C13r reversal and the normal polarity sample in Supplementary Figure S15C is only 2 cm above the reversal. Only the sample in the very middle of the reversal (Supplementary Figure S15D) has a poorly defined direction and large MAD angle, which is not unexpected because during reversals the geomagnetic field is much more weak and variable in direction than during stable polarity intervals.

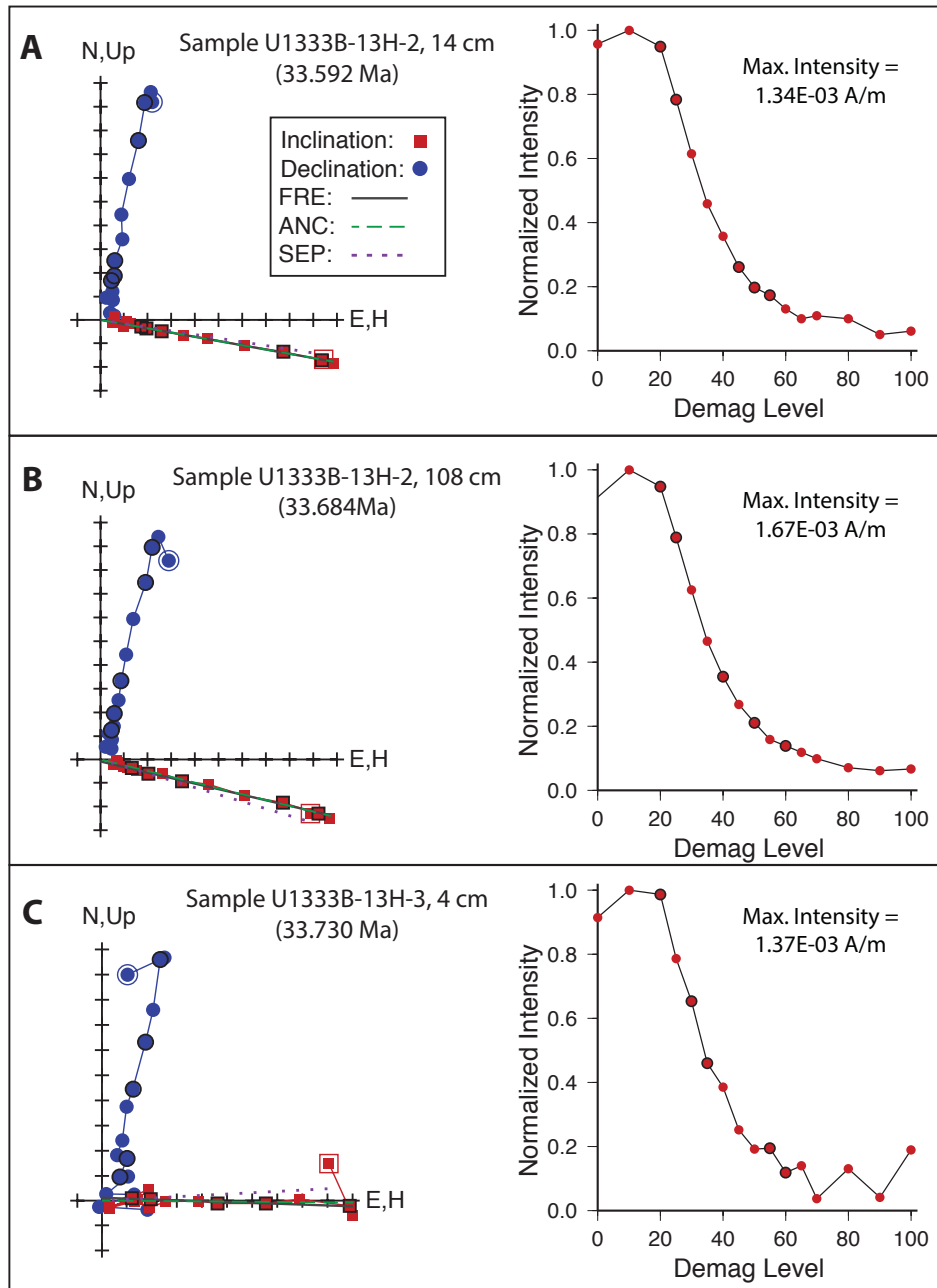


Figure 4a. (Fig. S15a of the supplement). Vector demagnetization diagrams and intensity decay plots for six intervals measured along U-channel samples that span the Chron C13n/C13r reversal. A) Sample U1333B-13H-2, 14 cm is a normal polarity sample 142 cm above the reversal, B) Sample U1333B-13H-2, 108 cm is a normal polarity sample 48 cm above the reversal, C) Sample U1333B-13H-3, 4 cm is a normal polarity sample 2 cm above the reversal, D) Sample U1333B-13H-3, 6 cm is a transitional sample in the very center of the Chron C13n/C13r reversal, E) Sample U1333B-13H-3, 9 cm is a reversed polarity sample 3 cm below the reversal, and F) Sample U1333B-13H-3, 90 cm is a reversed polarity sample 84 cm below the reversal.

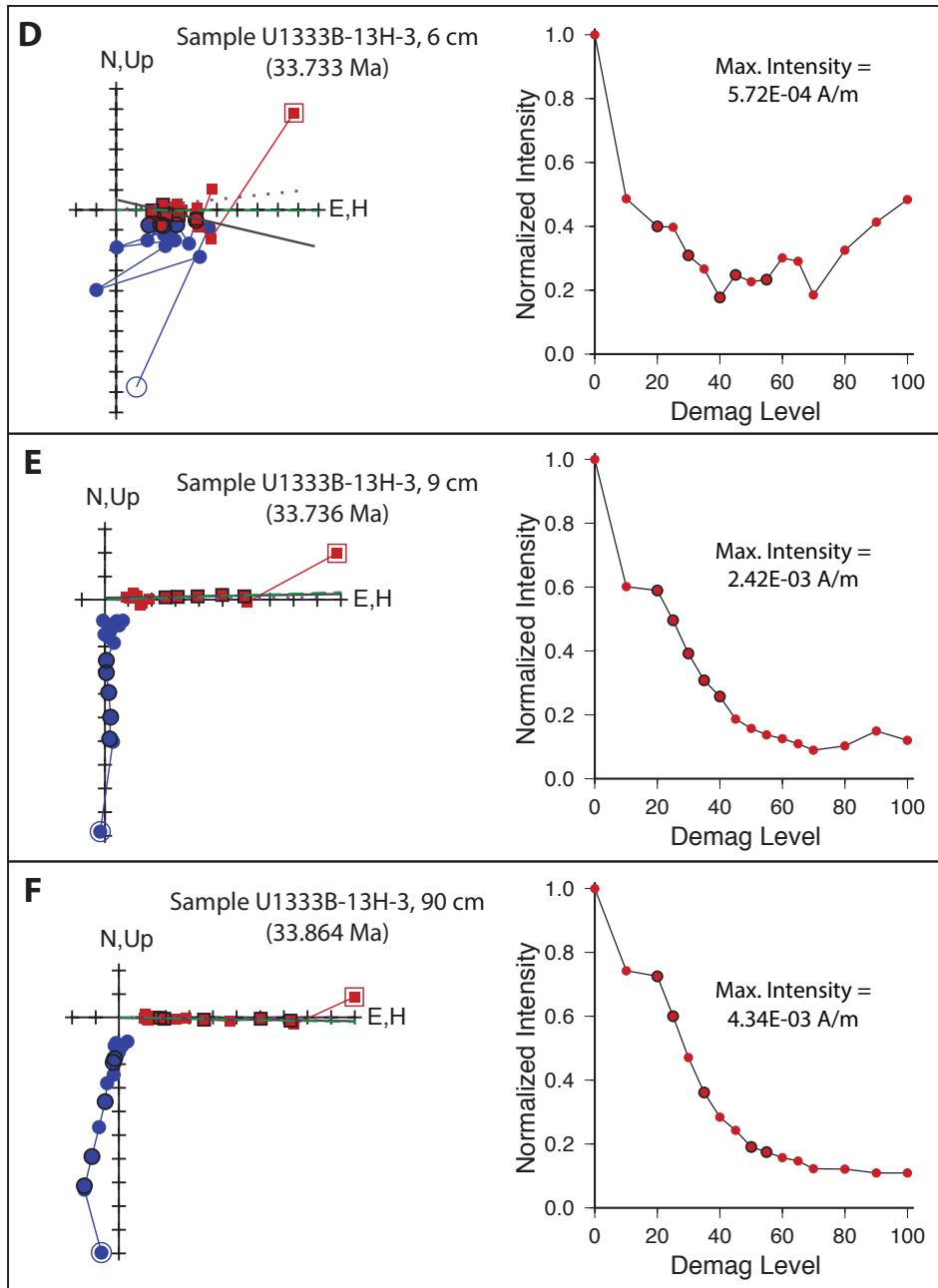


Figure 4b. – (Fig. S15b of the supplement) continued from pervious page.

Site 1052: The polarity stratigraphy at Site 1052 is referenced to Pälike et al. (2001). It is based on poor quality shipboard paleomagnetic data (ODP Leg 171B) (Shipboard Scientific Party, 1998) with support from shorebased work of Ogg and Bardot (2001). The magnetic stratigraphy at this site above C17r is very poor, and the black/white bars indicating polarity zones in Fig. 6 are misleading. At the very least, an assessment of the quality of the magnetostratigraphic record should be given, with complete referencing.

We assessed the quality of the magnetostratigraphic record, added the inclination data of Ogg and Bardot (2001) to Figure 6 (see Figure 5 of this reply) and completed the referencing for Site 1052. The following text is added to the chapter 4.3 Chron C15n to C17r – middle Priabonian to late Bartonian: “Although ODP Site 1052 has poor quality shipboard paleomagnetic data (Shipboard Scientific Party, 1998) shore-based work could identified the position of magnetochrons C16r, C17r and C18r (Ogg and Bardot, 2001; Fig. 6). After revision of the depth scale Pälike et al. (2001) re-evaluated the data and presented a more detailed magnetic stratigraphy spanning from C15r down to C18n.2n (Fig. 6). Because the shipboard data are of poor quality we consider the magnetic stratigraphy at 1052 only reliable for base C16n.2n, top C17n.1n, base C17n.3n and top C18n.1n based on the shore-based data of Ogg and Bardot (2001). The chron-boundary C15r/C16n.1n is likely documented around 12 rmcd in the 1052D shipboard data but not backed-up by shore based samples. Thus we assume that Chron C16 ends above ~14 rmcd.” In addition, ages and durations for unreliable chron boundaries as given in table 1 and 2 of the manuscript for Site 1052 are put in brackets and marked as uncertain. In Figure 9 of the manuscript (Comparison of magnetochron boundary ages and durations for Chron C12 to C19...) we only show the reliable chrons (base C16n, top and base C17n; and top C18n.1n).

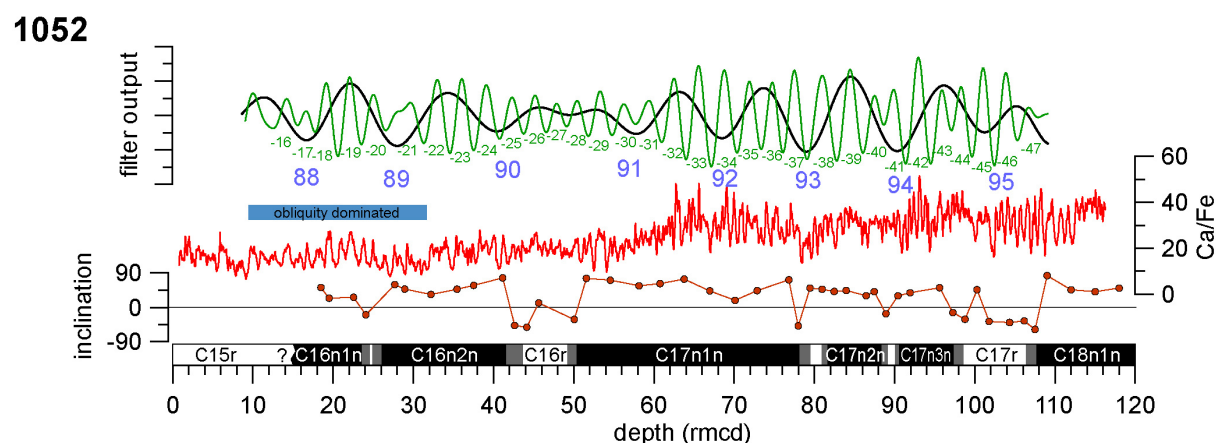


Figure 5. Cyclostratigraphy from Chron C15r to C18n.1n for ODP Site 1052 in the depth domain. Ca/Fe data, revised depth scale and paleomagnetic reversal pattern with errors from Pälike et al. (2001), inclination data from Ogg and Bardot (2001). Numbers represent the assigned short (green) and long (blue) eccentricity cycle maxima positions in the orbital solution (see supplementary Figure S8). Band pass filters: 405-kyr filter in black (0.09 ± 0.027 c/m); 100-kyr filter in green (0.32 ± 0.096 c/m). Please note the strong obliquity component present from 10 to 30 rmcd in the 1052 sedimentary record.

Site 1172: The polarity stratigraphy is referenced to Rohl et al. (2004) although it is actually documented in Fuller and Touchard (2004) and Touchard and Fuller (2004). Hole 1172D magnetic stratigraphy in the C17r to C18r interval is given in Fig. 7, although I do not see this interval documented in the Fuller/Touchard papers. The shipboard data magnetic stratigraphies in the relevant interval (Fig. F19, in Shipboard Scientific Party, 2001) indicates very poorly defined magnetic stratigraphy.

We apologize for a typo: 1172D is wrong, it should be 1172A. The typo is corrected now. Site 1172 magnetostratigraphy is indeed problematic and we address this in a new figure S10 to the supplementary material section (Figure 6 of this reply) and strong modification of the text in the manuscript. The following text is added to the chapter 4.4 *Chron C17r to C20n – Bartonian to late Lutetian*: “The shipboard data magnetic stratigraphies at ODP Site 1172 in the relevant interval (Fig. F19, in Shipboard Scientific Party, 2001) indicates poorly defined magnetic stratigraphy. Despite this difficulty Fuller and Touchard (2004) identified the positions of the top of C18n.1n, top of C18n.2n and base C18n.2n for Site 1172A. Subsequently the reversal pattern was slightly revised in Röhrl et al. (2004, see Fig. 6 therein) and used for cyclostratigraphy. Based on the shipboard inclination data (See Fig. S10) the top C18n.1n can be identified reliably. Base of C18n.1n and top of C18n.2n cannot be defined in 1172A based on these data. However, the compilation of bio-, chemo- and magnetostratigraphic data for the time encompassing the Middle Eocene Climate Optimum (MECO; Bohaty et al., 2009) shows that the distinct carbon isotope excursion (CIE) at the end of the MECO is close to the base of C18n.2n. Comparison of bulk stable carbon isotope data from 1172A (Bijl et al. 2010) with the magnetostratigraphy (Edgar et al., 2010) and bulk stable carbon isotope data of Site 1051 (Bohaty et al., 2009) (Fig. S10) suggests that the base of C18n.2n in 1172A should be indeed located at around 415 mbsf as proposed by Fuller and Touchard (2004). However the exact astronomical calibration of the base of C18n.2n using 1172A still needs to be refined by other records. Due to the good correlation of the CIE in the peak-MECO and the base of C18n.2n (Bohaty et al., 2009; Fig. S10) in various records a relatively good estimate for the duration of C18n altogether can still be achieved on the eccentricity level.”

In figure 7 of the manuscript we changed the magnetostratigraphy of 1172A as in reply-fig. 6 below indicating that only the top C18n.1n is reliable.

In essence no major change to the 405 kyr cyclostratigraphic framework is necessary.

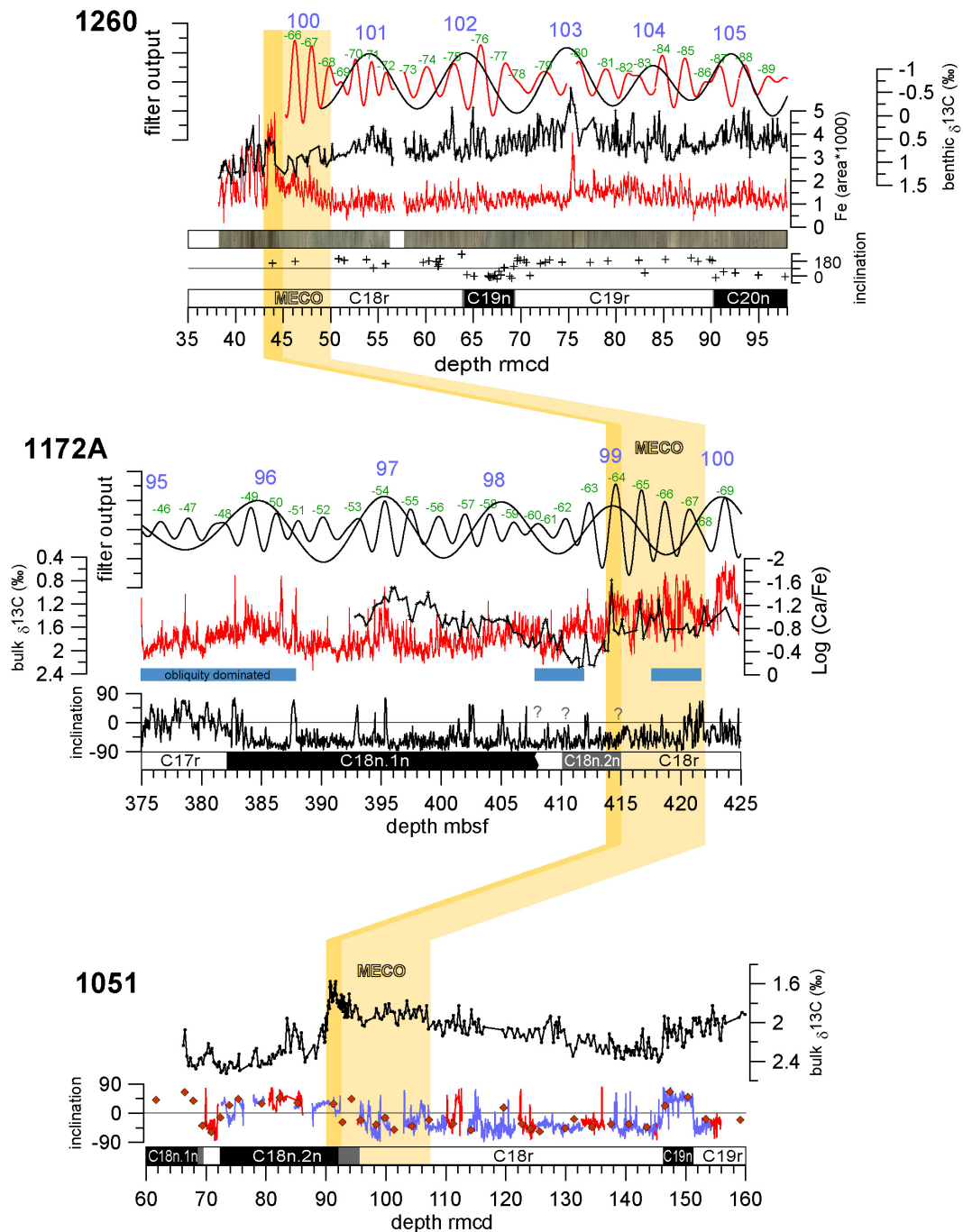


Figure 6. Correlation of the Middle Eocene Climate Optimum (MECO) between ODP Sites 1260 (Demerara Rise), 1172A (East Tasman Plateau) and 1051 (Blake Nose). For detailed caption of 1260 and 1172A data see Figure 7 (of the manuscript). Additional data: inclination data from discrete samples for 1260 (black crosses; Suganuma and Ogg, 2006; Edgar et al., 2007); for 1172A shipboard inclination data (black line; Shipboard Scientific Party, 2001) and the bulk stable carbon isotope data (Bijl et al., 2010). Data from 1051: Magnetostratigraphy and u-channel inclination data (1051A – red, 1051B – blue; Edgar et al. 2010), inclination from discrete samples (red diamonds; Ogg and Bardot, 2001), bulk stable carbon isotope data (black line with dots; Bohaty et al., 2009). The darker orange correlation band marks the carbon isotopes excursion (CIE) of the peak-MECO.

Site 1260: In Fig. 7, the C18r-C20r interval is indicated as black/white bars. The polarity stratigraphy is referenced to Westerhold and Rohl (2013), although it comes from the Shipboard Scientific Party (2004) and from Suganuma and Ogg (2006). The polarity designation in Suganuma and Ogg (2006) is based on a “polarity rating” from rotary cores where the viscous magnetic overprint is used to determine declination (and hence polarity) in these low paleolatitude (low inclination) data. The shipboard magnetostratigraphic data seem to be difficult to interpret in this interval.

To address this issue the following text is added to the chapter 4.4 Chron C17r to C20n – Bartonian to late Lutetian: “The magnetostratigraphy for ODP Site 1260 first was developed by the Shipboard Scientific Party (2004) and then refined by shore-based discrete samples (Suganuma and Ogg, 2006). Additionally Edgar et al. (2007) analyzed a total number of 100 samples at 20 - 30 cm resolution across each of the magnetic reversals using the same method of “polarity rating” from rotary cores where the magnetic overprint is used to determine declination (and hence polarity) in the low paleolatitude (low inclination) data.”

In Figure S10 (Fig. 6 of this reply) we added the data of Suganuma and Ogg (2006) and Edgar et al. (2007).

Without a full discussion of the magnetic stratigraphies, and the uncertainties associated with them, the astrochronological recalibrations of the GPTS cannot be evaluated. The stable isotope data, used in the astrochronologies, are available in the Pangaea database although these data are also not documented and referenced to Wilson et al. (unpublished).

We added the uncertainties (given in Tab. S16) and full discussion on the magnetostratigraphy of the different sites as reported above. The stable isotope data are archived in Pangaea (Tab. S13 & S14). These data do not include the data from the EOT because those are part of a different manuscript and need to be published with that manuscript (will be submitted early 2014), not here.

In summary, another updated calibration of the GPTS is not useful unless the data that are used are fully documented. This is not the case for the magnetostratigraphic or stable isotope data. As the magnetostratigraphies for Sites U1333, U1334 and 1218 are not independent, but “mapped in” from Site U1333 using the XRF data used to derive the astrochronologies, agreement in astrochronological ages of polarity reversals among the three sites is guaranteed.

As written in the manuscript our main objective is not to update the GPTS itself - this is a much bigger effort including many new deep sea records and even newly proposed expeditions – but to construct a cyclostratigraphic framework, develop a tuned age model for the PEAT sites and to define the position magnetostratigraphic boundaries in the 405-kyr cycle number scheme. To do so, we needed to include data from other sites available and thus are able to compare to previous estimates for the magnetostratigraphic boundaries. The study is important towards a new calibration of the GPTS in the future (as done in the GTS2012 for example) and for other scientists using the data from the PEAT records as well as Sites 1051, 1052, 1172A, 1260.

The agreement of 1218, U1333 and U1334 ages are due to the mapping of U1333 onto the other sites. We have discussed this above and stress here that the tuned magnetostratigraphy from U1333 alone is suitable to compare to other standard GPTS. Transferring the magnetostratigraphy (as also written in Westerhold et al. 2012) to the other sites enables to place biostratigraphy events within a paleomagnetic reference frame. This is of major importance for the calibration of biozones, and this can be independent from the absolute age (also discussed in Westerhold et al. 2012). All three sites show very similar records in different proxy data (see Fig 1, 2, 3 of this reply, the figures in the manuscript (Ca, Si, Fe and bulk stable isotope data) and Wilkens et al. 2013 as well as Westerhold et al. 2012) that can be correlated down to the cm level. Therefore we think it is appropriate to map the magnetostratigraphy from U1333 to 1218 and U1334.

Data are fully documented in the Pangaea data-base, pending isotope data of Wilson et al. will be available in Pangaea as well. We hope that the extensive tables S17, S18 and S19 containing the following U-channel paleomagnetic data are suitable to document good quality data:

Table information for tables S17, S18, S19 (as in the Pangaea data base): U-channel paleomagnetic data of IODP Hole 320-U1333A, B, C

#	Name	Short Name	Unit	Method	Comment
1	Sample code/label	Label			
2	Interval Cored	Cored	m		
3	DEPTH, sediment/rock	Depth	m		Geocode
4	Depth, composite	Depth c	mcd		based on Table 8 of Westerhold et al. (2012), CCSF-A
5	Depth, composite revised, adjusted	Depth adj rmcd	adj rmcd		based on Table 10 of Westerhold et al. (2012)
6	AGE	Age	ka BP		Geocode
7	Half	Half			working or archive half
8	Filter	Filter			data filter 1, If =0, data are suspect
9	Filter	Filter			data filter 2, If =0, data are suspect
10	Natural remanent magnetization	NRM	mT		no demagnetization, (AFD000)
11	NRM, Declination	Decl (NRM)	deg		no demagnetization, (Dec000)
12	NRM, Inclination	Incl (NRM)	deg		no demagnetization, (Inc000)
13	NRM, Intensity	Inten (NRM)	mA/m		NRM magnetization with no demagnetization, (Int000)
14	Natural remanent magnetization	NRM	mT		20 mT AF demagnetization, (AFD020)
15	NRM, Declination after demagnetisation	Decl (AF)	deg		20 mT AF demagnetization, (Dec020)
16	NRM, Inclination after demagnetisation	Incl (AF)	deg		20 mT AF demagnetization, (Inc020)
17	NRM, Intensity	Inten (NRM)	mA/m		NRM magnetization with 20 mT AF demagnetization (Int020)
18	Natural remanent magnetization	NRM	mT		25 mT AF demagnetization, (AFD025)
19	NRM, Declination after demagnetisation	Decl (AF)	deg		25 mT AF demagnetization, (Dec025)
20	NRM, Inclination after demagnetisation	Incl (AF)	deg		25 mT AF demagnetization, (Inc025)
21	NRM, Intensity	Inten (NRM)	mA/m		NRM magnetization with 25 mT AF demagnetization (Int025)
22	Natural remanent magnetization	NRM	mT		30 mT AF demagnetization, (AFD030)
23	NRM, Declination after demagnetisation	Decl (AF)	deg		30 mT AF demagnetization, (Dec030)
24	NRM, Inclination after demagnetisation	Incl (AF)	deg		30 mT AF demagnetization, (Inc030)
25	NRM, Intensity	Inten (NRM)	mA/m		NRM magnetization with 30 mT AF demagnetization (Int030)
26	Natural remanent magnetization	NRM	mT		40 mT AF demagnetization, (AFD040)
27	NRM, Declination after demagnetisation	Decl (AF)	deg		40 mT AF demagnetization, (Dec040)
28	NRM, Inclination after demagnetisation	Incl (AF)	deg		40 mT AF demagnetization, (Inc040)
29	NRM, Intensity	Inten (NRM)	mA/m		NRM magnetization with 40 mT AF demagnetization (Int040)
30	Natural remanent magnetization	NRM	mT		50 mT AF demagnetization, (AFD050)

31	NRM, Declination after demagnetisation	Decl (AF)	deg		50 mT AF demagnetization, (Dec050)
32	NRM, Inclination after demagnetisation	Incl (AF)	deg		50 mT AF demagnetization, (Inc050)
33	NRM, Intensity	Inten (NRM)	mA/m		NRM magnetization with 50 mT AF demagnetization (Int050)
34	Natural remanent magnetization	NRM	mT		60 mT AF demagnetization, (AFD060)
35	NRM, Declination after demagnetisation	Decl (AF)	deg		60 mT AF demagnetization, (Dec060)
36	NRM, Inclination after demagnetisation	Incl (AF)	deg		60 mT AF demagnetization, (Inc060)
37	NRM, Intensity	Inten (NRM)	mA/m		NRM magnetization with 60 mT AF demagnetization (Int060)
38	Natural remanent magnetization	NRM	mT		80 mT AF demagnetization, (AFD080)
39	NRM, Declination after demagnetisation	Decl (AF)	deg		80 mT AF demagnetization, (Dec080)
40	NRM, Inclination after demagnetisation	Incl (AF)	deg		80 mT AF demagnetization, (Inc080)
41	NRM, Intensity	Inten (NRM)	mA/m		NRM magnetization with 80 mT AF demagnetization (Int080)
42	Inclination	Incl	deg	Principal component analyses (PCA)	free-fitting option
43	Declination	Decl	deg	Principal component analyses (PCA)	free-fitting option
44	Maximum angular deviation	MAD	deg	Principal component analyses (PCA)	free-fitting option
45	Length of principal axis	Length	mA/m	Principal component analyses (PCA)	free-fitting option
46	Deviation angle	Deviation	deg	Principal component analyses (PCA)	deviation of best-fitting line from origin, free-fitting option
47	Number of steps	N steps	#	Principal component analyses (PCA)	number of demagnetization steps used to fit the PCA line, free-fitting option
48	Demagnetization step	Demag step	mT	Principal component analyses (PCA)	lowest demagnetization step used, free-fitting option
49	Demagnetization step	Demag step	mT	Principal component analyses (PCA)	highest demagnetization step used, free-fitting option
50	Inclination	Incl	deg	Principal component analyses (PCA)	line anchored to origin
51	Declination	Decl	deg	Principal component analyses (PCA)	line anchored to origin
52	Maximum angular deviation	MAD	deg	Principal component analyses (PCA)	line anchored to origin
53	Length of principal axis	Length	mA/m	Principal component analyses (PCA)	line anchored to origin
54	Deviation angle	Deviation	deg	Principal component analyses (PCA)	deviation of best-fitting line from origin, line anchored to origin
55	Number of steps	N steps	#	Principal component	number of demagnetization steps used to fit the PCA line anchored to origin

				analyses (PCA)	
56	Demagnetization step	Demag step	mT		lowest demagnetization step used, line anchored to origin
57	Demagnetization step	Demag step	mT		highest demagnetization step used, line anchored to origin
58	Inclination	Incl	deg		stable end point (SEP) inclination, a Fisherian mean
59	Declination	Decl	deg		stable end point (SEP) declination, a Fisherian mean
60	Precision parameter	k			Fisherian precision parameter for SEP
61	Number of steps	N steps	#		number of demagnetization steps used for SEP
62	Angular distance	Angular dist	deg		between PCA direction (free-fitting) and SEP direction
63	Declination	Decl	deg		mean declination for a drill core
64	Declination	Decl	deg		reorientation correction dependent on half from which sample was collected
65	Declination	Decl	deg		other reorientation correction related to sample handling
66	Declination	Decl	deg		sum of several reorientation corrections
67	Declination	Decl	deg		reoriented to approximate mean geographical coordinate
68	Declination	Decl	deg		correction for within-core rotation that occurs as core is collected
69	Declination	Decl	deg		preferred after all corrections have been applied
70	Polarity	Polarity			geomagnetic polarity (R=Reversed, N=Normal, T=Transitional, X=Uncertain)
71	Chronozone	Chronozone			polarity chron age of sample